Original Research Paper

Calibration of the cloud and aerosol spectrometer for coal dust composition and morphology

T.L. Barone [a],*, E. Hesse [b], C.E. Seaman [a], A.J. Baran [c,b], T.W. Beck [a], M.L. Harris [a], P.A. Jaques [d], T. Lee [a], S.E. Mischler [a]

[a] Pittsburgh Mining Research Division, National Institute for Occupational Safety and Health, Centers for Disease Control and Prevention, 626 Cochrans Mill Road, Pittsburgh, PA 15236, United States
[b] School of Physics, Astronomy and Mathematics, University of Hertfordshire, College Lane, Hatfield, Herts AL10 9AB, United Kingdom
[c] Met Office, Fitzroy Road, Exeter EX1 3PB, United Kingdom
[d] California Department of Public Health, PO Box 997377, MS 0500, Sacramento, CA 95899-7377, United States

ABSTRACT

The cloud and aerosol spectrometer (CAS) was calibrated to enable CAS sizing of coal dust for studies on flammable dust control. Coal dust sizes were determined by light-scattering theories for irregular particles that account for particle composition and morphology in computing coal dust diameters. Coal dust size computations were compared with test dust that was generated by cyclone separation and air-jet sieving and characterized by aerodynamic particle sizer (APS) and computer-controlled scanning electron microscopy (CCSEM) measurements. For test dust in the range of 0.5–32 μm, coal dust size distributions were consistent with cyclone-separated and sieve-segregated sizes. For the 3–20 μm size range, the coal dust size distribution had a mass median diameter that was 14% larger than that of the APS. This difference was reasonable considering that the basic calibration for glass spheres had 13% uncertainty. For the 20–32 μm and 32–45 μm test dusts, mass median diameters differed from CCSEM measurements by only 4% and 5%, respectively. Overall, the results suggest agreement between test dust sizes and computations for coal dust. Alternatively, using conventional Mie theory computations for spheres, coal dust mass median diameters were 35% and 40% larger than APS and CCSEM measurements, respectively.

Published by Elsevier B.V. on behalf of The Society of Powder Technology Japan. All rights reserved.

1. Introduction

In 2010, an explosion in an underground mine led to the death of 29 coal miners in the eastern United States [1]. The disaster was caused in large part by the explosion of coal dust [1]. Coal dust generated by mining equipment became a source of fuel for the explosion after being deposited and accumulating on underground mine surfaces. To prevent such an explosion, coal dust on mine surfaces should be adequately treated with incombustible dust [2]. In addition, coal dust can be removed from mine air before it deposits and accumulates on mine surfaces [3,4].

Coal dust can be removed from mine air by using control technologies such as wet scrubbers [3,4] and water sprays [5]. The effectiveness of these control technologies can be determined by measuring the particle size distribution (PSD) upstream and downstream of their application. Measuring the PSD is important in efforts to prevent dust explosions because particle size influences coal dust flammability and explosibility [6]. Flammability generally decreases with increasing particle size although this depends on particle chemical composition and other factors. For a composition with significant volatile matter, such as bituminous coal, particles are flammable in the size range of 0.5–50 μm [6,7]. PSDs in this size range can be measured using optical instruments that detect particle light scattering. However, measuring the PSD of coal dust is challenging because of its irregular morphology and light-absorbing properties. Since most optical instruments are calibrated for spherical particles with weak light-absorbing properties, the calibrations are not applicable to coal dust [8].

To measure the PSD of coal dust, optical instruments should be calibrated for coal dust's specific composition and morphology. Calibrations for composition are made by including measurements for particle refractive index in light-scattering computations [9]. Without calibrations for particle refractive index, coal dust size can be underestimated by a factor of 5 by optical instruments [10,11]. One optical instrument often calibrated for refractive

Nomenclature

Abbreviations

CAS	cloud and aerosol spectrometer
APS	aerodynamic particle sizer
CCSEM	computer-controlled scanning electron microscopy
PSD	particle size distribution
LD	laser diffraction particle sizer
RTDF	ray tracing with diffraction on facets
SSPD	small-scale powder disperser
HEPA	high-efficiency particulate arrestor

Latin symbols

d_a	aerodynamic diameter [μm]
d_{ev}	equivalent volume diameter [μm]
d_p	particle diameter [μm]
d_{pa}	projected area equivalent diameter [μm]

k	imaginary part of refractive index [–]
k_e	parameter that depends on particle angularity [–]
k_v	volume shape factor [–]
m	refractive index [–]
m_a	flakiness aspect ratio [–]
n	real part of refractive index [–]
N	total particle number [number]
n_a	elongation aspect ratio [–]
V%	percent of total particle volume [percent]

Greek symbols

χ	dynamic shape factor [–]
ρ_0	unit density [kg/m³]
ρ_p	particle inherent density [kg/m³]

index is the laser diffraction particle sizer (LD) [12–15]. LDs are often used in conjunction with classical Mie theory [16,17] to estimate particle diameter based on light-scattering measurements from an ensemble of particles and are suitable for spherical particles and powders that are easily dispersed. However, LDs may not be adequate for coal dust because of its irregular morphology [18,19] and tendency to agglomerate [20]. Although methods to compensate for the effects of morphology have been investigated [15,21,22], most commercially available LDs do not include the sensing and analysis tools required to calibrate for irregular morphologies [12]. Including morphology effects is important in estimating particle diameter because assuming spherical shapes of particles has led to inaccuracies in sizing irregular particles [23,24]. The improper assumption of spherical shapes can lead to the overestimation of coal dust diameter and consequently to the underestimation of coal dust flammability and explosibility. For instance, if light scattered from the facets and cross section of an irregular particle is entirely attributed to the cross section of a spherical particle, the equivalent volume diameter can be overestimated. An overestimation of diameter can lead to the underestimation of the specific surface area available for interaction with an oxidizing atmosphere and consequently to the underestimation of flammability.

Particle morphology and composition effects can be included in PSD estimates by calibrating single-particle optical spectrometers (or optical particle counters). Single-particle measurements can be predicted using fundamental light-scattering theories that contain realistic models for particle morphology and measurements for particle refractive index [25,26]. These models are used to relate particle forward light-scattering measurements to particle diameter. In prior research, one type of single particle optical spectrometer—the cloud and aerosol spectrometer (CAS) [27,28]—was successfully calibrated for irregular particle morphology and composition. Specifically, the CAS was calibrated by applying ray tracing with diffraction on facets (RTDF) and T-matrix theories to compute PSDs for volcanic ash, which, like coal, has irregular morphology [29]. RTDF theory was applied to large (1.5–50 μm) irregular particles [30], and T-matrix theory [31] was applied to submicron and micron size irregular particles. Using RTDF and T-matrix theories, PSDs can be estimated based on size- and shape-dependent light-scattering properties.

In the current work, T-matrix and RTDF theories were applied to estimate coal dust size distributions by analyzing the light scattering of particles over sub-1.5 μm and 1.5–50 μm size ranges, respectively. The estimated particle size distributions were compared with test dust size ranges. For the comparison, (1) bulk dust was size-segregated by cyclone separation and air-jet sieving, (2) size-segregated dust was dispersed and de-agglomerated by using a modified small-scale powder disperser, and finally (3) particle size distributions of the coal dust were characterized by aerodynamic particle sizer (APS) and computer-controlled scanning electron microscopy measurements (CCSEM). Size ranges indicated by cyclone separation and air jet sieving and PSDs determined by the APS and CCSEM were compared with those determined by CAS measurements and T-matrix and RTDF theory computations.

2. Methods

The raw measurements of the CAS (analog to digital converter counts) were converted to a relevant metric (particle optical scattering cross section) by calibrating with glass sphere standards and classical Mie theory [16,17]. After the conversion, particle scattering cross section measurements were related to coal dust diameters (equivalent volume) by calibrating with T-matrix and RTDF theories. Coal dust diameters determined from the calibration were compared with test dust size ranges produced by cyclone separation (sub-2 μm) and air-jet sieving (3–20 μm, 20–32 μm, and 32–45 μm). The sizes selected by air-jet sieving were determined by the sizes of standard test sieves (ASTM E11 and ISO 565/3310-1) and the cyclone retention efficiency (Section 2.4). Coal dust size distributions were also compared with test dust measurements by the APS (Model 3321, TSI Inc., MN) and CCSEM (PSEM Express, ASPEX, PA). Following the evaluation of the calibration, CAS measurements for bulk dust were compared with conventional LD measurements (Model LS 13 320, Beckman-Coulter, CA). Quantification of CAS counting efficiencies and coincidence errors was beyond the scope of the current study, considering previous conflicting results [32,33].

2.1. CAS calibration with glass spheres

Glass spheres were dispersed and transferred to the CAS using the sampling system described in Section 2.5. In the CAS, particles passing through a 120-μm beam width were detected and processed. The forward light-scattering detector (4°–12°) gave a voltage signal, which was sampled by a high-gain and a low-gain analog-to-digital (A/D) converter (output is counts). The counts value for a single particle is proportional to the optical scattering cross section. The manufacturer-recommended proportionality

constant (4521) was used for the high-gain A/D converter. This was applied to coal dust ≤ 2.3 μm, which corresponded to 15,000 counts (conservative value before A/D saturation).

For particles >2.3 μm, the proportionality constant between A/D counts and optical scattering cross section was measured using glass sphere standards. For each glass sphere standard, the counts distribution was fitted with a normal curve, and the mode was divided by the scattering cross section from Mie theory [16,17]. This was done for National Institute of Standards and Technology traceable glass sphere standards with nominal diameters of 5 μm (5.4 ± 0.7 μm), 10 μm (10.0 ± 1.1 μm), 15 μm (15.9 ± 1.6 μm), 20 μm (18.2 ± 1.8 μm) (borosilicate, SPI Supplies, PA), and 30 μm (31.33 ± 0.82 μm) (soda-lime, Whitehouse Scientific, UK). The sizes of the glass spheres were selected to be consistent with the range of interest for coal dust and were determined by the available sizes of certified standards. The counts value for each coal dust particle was divided by the average proportionality constant to determine a particle optical scattering cross section.

2.2. Light-scattering theories for irregular particles

Particle optical scattering cross section measurements were related to coal dust diameters by RTDF theory. RTDF theory describes light-scattering patterns for complex particles, which have sizes outside the domain of conventional methods (1.5–50 μm) [30]. It differs from conventional geometric optics by considering diffraction at surface planes (facets) in addition to diffraction at the projected cross section and therefore describes the size and shape dependence more effectively. The faceted shape was approximated by using the distorted triadic Koch fractal as described in Macke et al. [34] (Fig. 1a). The fractal-like morphology should provide a more realistic representation of coal dust than spheroids as indicated by the representative particle in Fig. 1b. During RTDF computations, facets were randomly tilted [34] because this provides an effective smoothing of the surface as well as a randomization of overall particle shape. This approximation provided better representation of the surface of the coal dust, which is indicated by the representative particle in Fig. 1b.

To determine whether coal dust morphology should be modeled as compact or elongated in RTDF theory computations, aspect ratio was measured by CCSEM (Section 2.7). Aspect ratio was defined as the maximum particle diameter divided by the diameter perpendicular to the maximum. For a given particle volume, specifying an aspect ratio greater than 1 would result in an increase in particle optical scattering cross section. This is because the greater-than-1 aspect ratio approximation would lead to an increased particle cross-sectional area per unit volume for the irregular particles compared to spheres. An increase with deviation from compact particle geometry is expected, because the orientation averaged projected cross section increases for a given particle volume. This increase would require assigning smaller equivalent volume sphere diameters to the particles with a projected area aspect ratio more than 1 (which are assumed to be elongated (see Section 3.1)) relative to that of compact particles. The effect of aspect ratio on coal dust size computations is given in Section 3.1.

Smaller particles (0.5–1.5 μm) were modeled by T-matrix theory, for which dust morphology was represented as hexagonal cylinders with aspect ratio unity (the aspect ratio is defined here as the cylinder height to diameter) [31]. Application of T-matrix theory for ≤1.5-μm irregular particles and RTDF theory for >1.5-μm irregular particles was previously carried out to estimate light-scattering properties for irregularly shaped particles—volcanic ash [29] and mineral dust aerosols [35].

2.3. Coal dust refractive index

A bituminous coal with low volatile content (Pocahontas No. 3) was used for the current study. Its refractive index has a mid-range value relative to other coal types [36]. The refractive index (m = n − ik) is an important property in equations for particle light scattering and absorption. Light absorption is closely related to the imaginary part of refractive index (k), but it is also affected by the real part (n) [37]. The imaginary part is relatively high for coal dust and was included in forward light-scattering computations. Both the real and imaginary values (1.85–0.23i) are close approximations for the current study because these were measured at wavelength 650 nm, while the CAS measurement was at 658 nm.

2.4. Test dust generation

Sieving is a conventional method for size-segregating coarse dust but becomes challenging when the majority of particles are strongly agglomerated or electrostatically charged [38]. Because electrostatic charging was problematic for the type of bituminous coal dust used in the current study [39], an air-jet sieve (Hosokawa Micron Powder Systems, Summit, NJ) [38] was used. In the air-jet sieve, a single sieve screen was loaded with a few grams of dust, a stream of air rotated below the sieve lifting dust from the screen, and a high-flow rate vacuum pump pulled dust through the screen. The dust-laden air was passed through a conductive tube at high
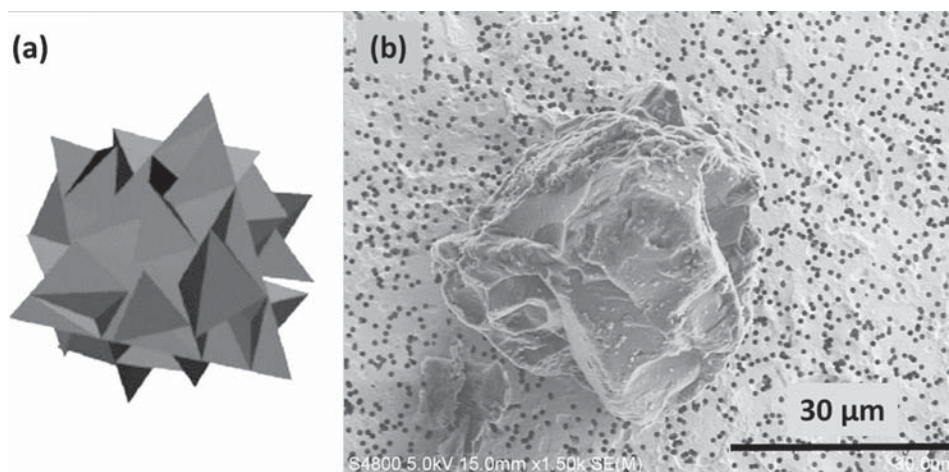

Fig. 1. (a) Distorted fractal-like crystal. This crystal shape was randomized to model an irregular particle with rough surface. (b) Bituminous coal dust with smoother surface.

air velocity (44 m/s) into a cyclone (Hosokawa Alpine, Germany) for collection in the cyclone grit pot. Using this system, coal dust in the following size ranges was collected: (1) 3–20 µm, (2) 20–32 µm, and (3) 32–45 µm. The lower size of 3 µm was determined by measuring the cyclone retention efficiency for glass spheres. Particles with diameters greater than or equal to 3 µm were completely retained.

Smaller test dust was generated by using the above cyclone to size-separate particles from bulk dust. This was done by operating the cyclone between the dust disperser and CAS as shown in Fig. 2, so that small particles penetrating the cyclone were transferred to the CAS. Transfer tubes that matched the inlet characteristics of both the cyclone and the CAS were used with external couplers to reduce particle inlet losses. The cyclone penetration efficiency for the CAS flowrate was determined using glass spheres. The penetration efficiency decreased sharply for particles larger than 2 µm, with 50% of 2.1 µm and 10% of 2.5 µm penetrating. These measurements gave the nominal sub-2 µm test dust size range and are shown alongside coal dust measurements in Section 3.3.

2.5. Test dust de-agglomeration for CAS measurements

In preparation for CAS analysis, test dust was dispersed and de-agglomerated by a modified small-scale powder disperser (SSPD) (Model 3433, TSI, MN) [40]. The SSPD was modified by changing the flow path downstream of the Venturi aspirator, so that the total flow leaving the aspirator was transferred with a straight vertical tube into the CAS inlet to minimize losses. The SSPD was operated with 2 L/min capillary flow, which sampled dust from a turntable platform; and with 28 L/min sheath flow, which de-agglomerated particles in the Venturi aspirator.

Coal dust was sampled, de-agglomerated, and transferred to the CAS using a straight and non-narrowing flow path to prevent particle losses from interception and impaction (Fig. 3). The CAS and SSPD were aligned vertically to prevent particle settling along the flow path. Dust dispersed by the SSPD was introduced to the CAS along with high flow rate (1.5×10^3 L/min), high-efficiency particulate arrestor (HEPA)-filtered air to avoid particle settling and background particle interferences. Irregular flow patterns from large-scale turbulence were avoided by operating two HEPA filters (Omnitec Design, Inc., Mukilteo, WA) at half-capacity and counter-current to each other to balance the flow.

Coal dust de-agglomeration by the SSPD was evaluated to determine whether test dust was adequately prepared for single-particle analysis by the CAS. If powders were not adequately de-

Fig. 2. Diagram of how coal dust was dispersed by the modified SSPD, size-separated by the high flow rate cyclone, and how sub-2 µm particles were introduced to the CAS.

agglomerated, test dust measured by the CAS would be larger than sizes selected by air-jet sieving. To evaluate SSPD de-agglomeration, samples were collected by gravitational settling in a small stainless steel chamber (5-cm-diameter) on a 13-mm-diameter stage for CCSEM analysis (Section 2.7). The mass of the dust was varied to obtain an adequate deposit without particle overlap from over-sampling, and the results are given in Section 3.1.

2.6. Test dust measurements by APS

Samples were de-agglomerated for APS measurements as with the CAS measurements, but the total flow could not be transferred because the APS flow rate (5 ± 0.05 L/min) is smaller than that of the modified SSPD (30 ± 0.2 L/min). Samples were transferred while minimizing distortion of the size distribution by sampling the total flow with an isokinetic probe (0.58 ± 0.02 cm inner diameter), which allowed for approximate matching of the total and partial flow velocities (within 5%) (Fig. 4).

The APS distribution was based on aerodynamic diameter (d_a), while the CAS distribution was based on equivalent volume diameter (d_{ev}). The two distributions can be placed on the same diameter basis by using information on particle density (ρ_p) and the dynamic shape factor (χ) [41]:

$$d_a = d_{ev}\left(\frac{\rho_p}{\rho_0\chi}\right)^{\frac{1}{2}} \tag{1}$$

where ρ_0 is unit density by definition of d_a. Dynamic shape factor was previously reported for bituminous coal dust [42], and an average of previous measurements (1.08) was used. Density was previously measured for the type of bituminous coal used in the current study (1.37 g/cm^3) [43]. As conventionally done, a correction for particle density [44] was applied to APS measurements. Subsequently, APS measurements of d_a were placed on a d_{ev} basis using Equation (1).

2.7. Test dust measurements by CCSEM

Coal dust PSDs were measured for particles >10 µm by CCSEM analysis [45–48]. The CCSEM (PSEM Express™, ASPEX, PA) provided an automated measurement process for particle sizing and counting by way of a backscatter electron detector (BSED). The BSED contrast resulted from atomic number differences in the particle sample and the background substrate. Contrast was established for sample particles relative to the background material by using a track-etch polycarbonate filter with gold coating (Whatman 800195, GE Life Sciences, Pittsburgh, PA).

Samples were prepared in a dilute slurry in isopropanol and de-agglomerated in an ultrasonic bath for 1 h. The slurry was agitated by a vortex mixer while being pipetted onto the gold-coated filter. The sample was mounted in a glass filter holder and vacuum filtered. Filter samples were placed on aluminum stubs with conductive carbon tape. Particles were analyzed at 100–250 times magnification and 20 keV to determine projected area diameter. About 3500 particles were analyzed for each 20–32 µm and 32–45 µm powder. CCSEM measurements were in agreement with particle diameters measured manually using ImageJ software (National Institutes of Health, MD) (Fig. 5; root mean square error 3 µm).

The CCSEM distributions were based on projected area diameter (d_{pa}), while the CAS distribution was based on equivalent volume diameter. Equivalent volume diameter can be estimated from projected area diameter using the volume shape factor. The volume shape factor was measured previously for bituminous coal dust, but the values corresponded to longer aspect ratios (2–3) [42] than
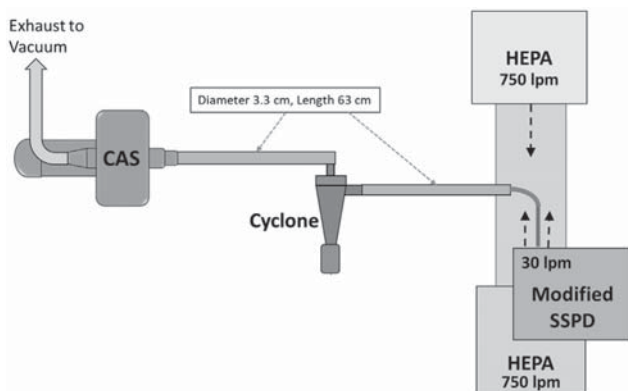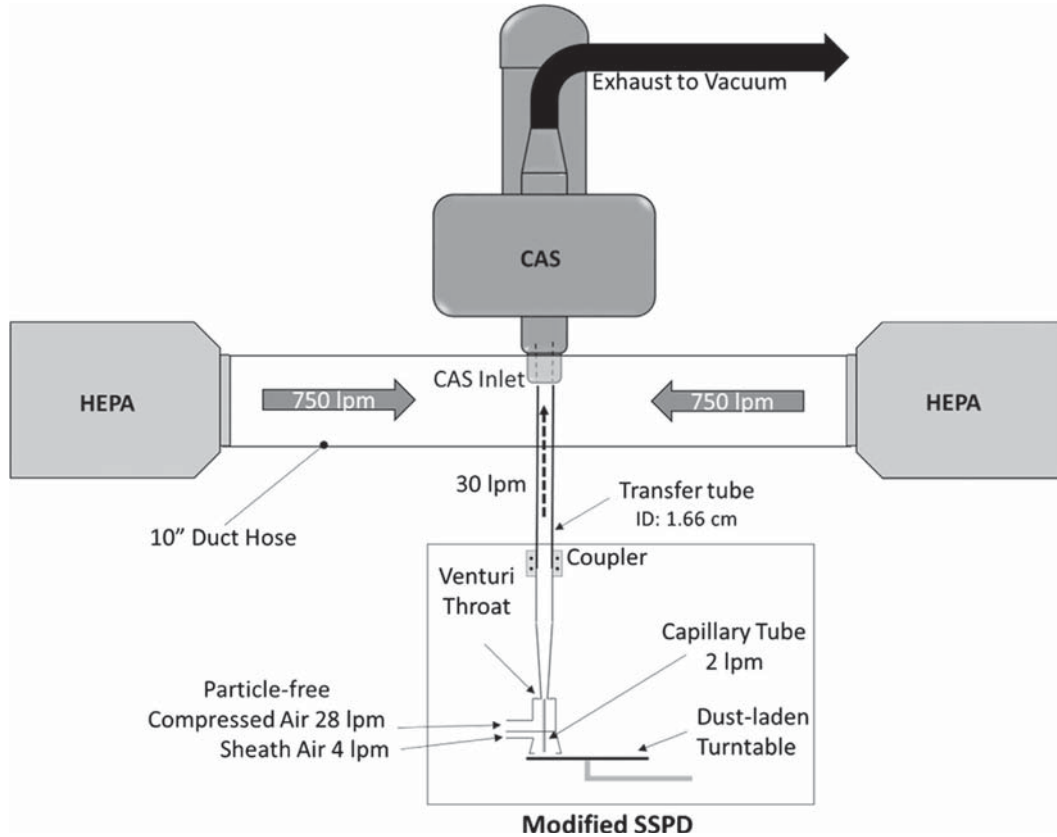
Fig. 3. Diagram of how test coal dust (3–20 μm, 20–32 μm, 32–45 μm) was dispersed by the modified SSPD and introduced to the CAS.
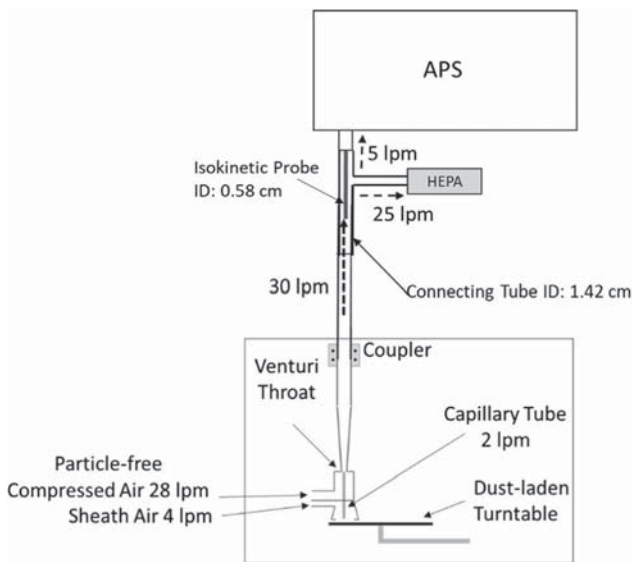

Fig. 4. Diagram of how test coal dust (3–20 μm) was dispersed by the modified SSPD and introduced to the APS.
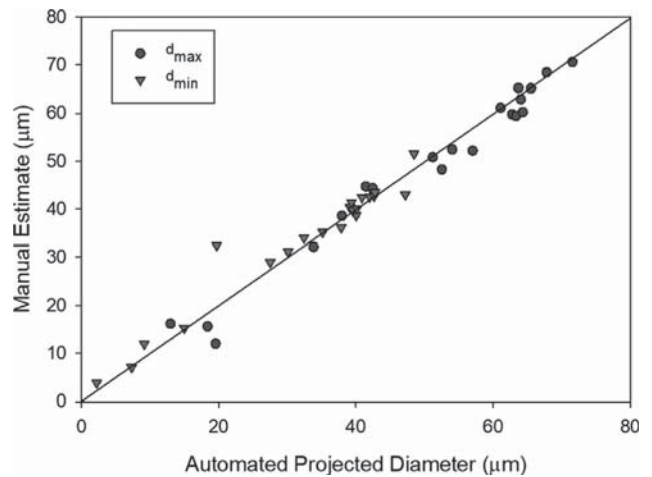

Fig. 5. Comparison of maximum (d_{max}) and minimum (d_{min}) coal dust diameters estimated manually using ImageJ software and by automated feature analysis with the CCSEM. Line represents 1:1.

measured in the current study (Section 3.1). However, a general expression can be used that allows for the calculation of the volume shape factor (k_v) with aspect ratio as a variable [42]:

$$k_v m_a \sqrt{n_a} = k_e \qquad (2)$$

where n_a is the elongation aspect ratio, m_a is the flakiness aspect ratio, and k_e is a value that depends on particle angularity. A value of 0.43 was used as an intermediate k_e for particles between tetrahedral and smooth shapes as done previously [42]. The aspect ratio for flakiness was assumed to be 1 based on 3-D measurements for pulverized bituminous coal dust [49] and the results of Timbrell [50]. Using Equation (2), the volume shape factor was 0.37 as defined by Hinds [41] and indicates that d_{ev} should be 11% smaller than d_{pa}. Using this value, CCSEM distributions were converted to a d_{ev} basis. This allowed for direct comparison of CAS- and CCSEM-measured size distributions for coal dust.

3. Results and discussion

3.1. Coal dust morphology and De-Agglomeration

Coal dust was de-agglomerated to allow a relevant comparison between test dust diameters and CAS measurements. De-agglomeration was evaluated after dispersing samples with the modified SSPD. The sample mass dispersed by the SSPD was varied (while feed rate was fixed) to determine the mass which minimized particle overlap on the sample substrate to avoid artifact agglomerates. Dispersing 0.5 mg led to the collection of an adequate number of particles and minimized particle overlap, as indicated by the comparison of deposition patterns for dust samples of 0.5 mg and 1.0 mg in the low-magnification CCSEM image in Fig. 6. Higher-magnification CCSEM images were evaluated manually and it was determined that 98.5% were single particles while the remainder were doublets. Agglomerates of three or more particles were absent. These results suggested that the modified SSPD adequately dispersed samples for analysis by the CAS.

Coal dust morphology was represented as a faceted shape in RTDF theory computations. To determine whether the faceted shape should be modeled as compact or elongated, aspect ratio was measured by CCSEM. On average, coal dust was elongated with an aspect ratio of 1.36 ± 0.18. The elongated aspect ratio approximation led to an increased particle cross-sectional area per unit volume for the irregular particles compared to spheres. An increase with deviation from compact particle geometry is expected, since the orientation averaged projected cross section increases for a given particle volume. Elongated particles were assumed to be randomly oriented since the flow was highly turbulent (CAS velocity 25 m/s and Reynolds number 5×10^4) [51]. This consideration of aspect ratio led to assigning slightly smaller equivalent volume diameters (2%) in estimating coal dust size distributions. This size shift corresponded to about a 6% decrease in volume.

3.2. CAS calibration with glass spheres

The CAS was calibrated by using glass sphere standards to determine the proportionality constant between the CAS response (analog-to-digital converter counts) and particle optical scattering cross section. This was needed to determine the optical scattering cross section for coal dust, which was subsequently analyzed by T-matrix and RTDF theories to determine coal dust diameter. Exam-
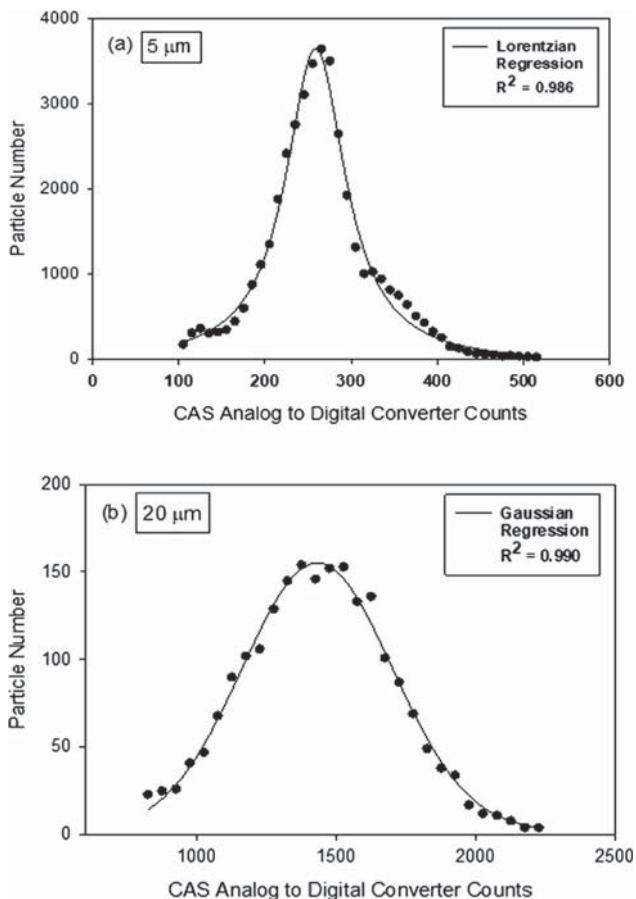

Fig. 7. Distribution of glass spheres measured by the CAS low-gain A/D converter for the nominal (a) 5-μm and (b) 20-μm standards. Glass spheres standards were sampled using the system in Fig. 3.

ple response distributions are shown for the 5-μm and 20-μm standards in Fig. 7. Although these distributions are well defined, others had more ambiguous peaks [52], which contributed to the measurement uncertainty. Based on the results for all standards, the average proportionality constant was 32.4 ± 4.2 (13%; two standard deviations). Thus, an uncertainty of at least 13% can be expected for coal dust optical scattering cross section. Factors con-
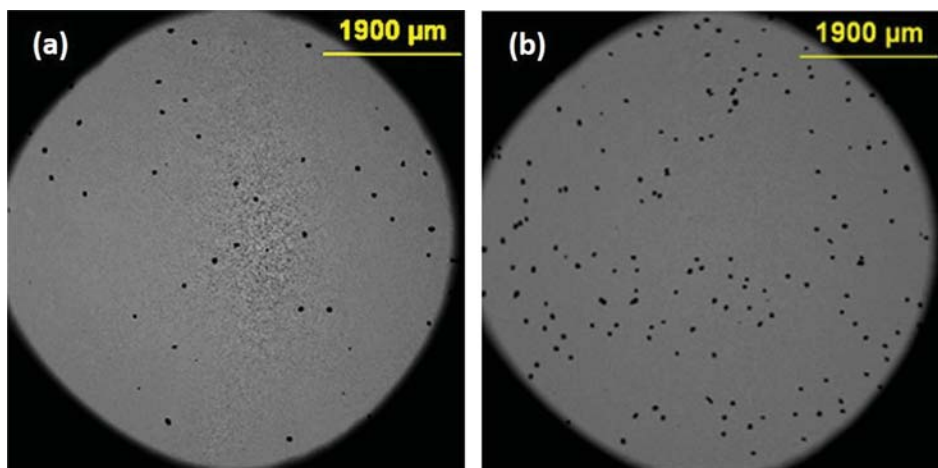

Fig. 6. Deposition pattern of coal dust collected for the evaluation of de-agglomeration. Masses of (a) 0.5 mg, and (b) 1.0 mg were sampled and dispersed by the modified SSPD with 2 L/min capillary and 28 L/min aspirator flow rates.
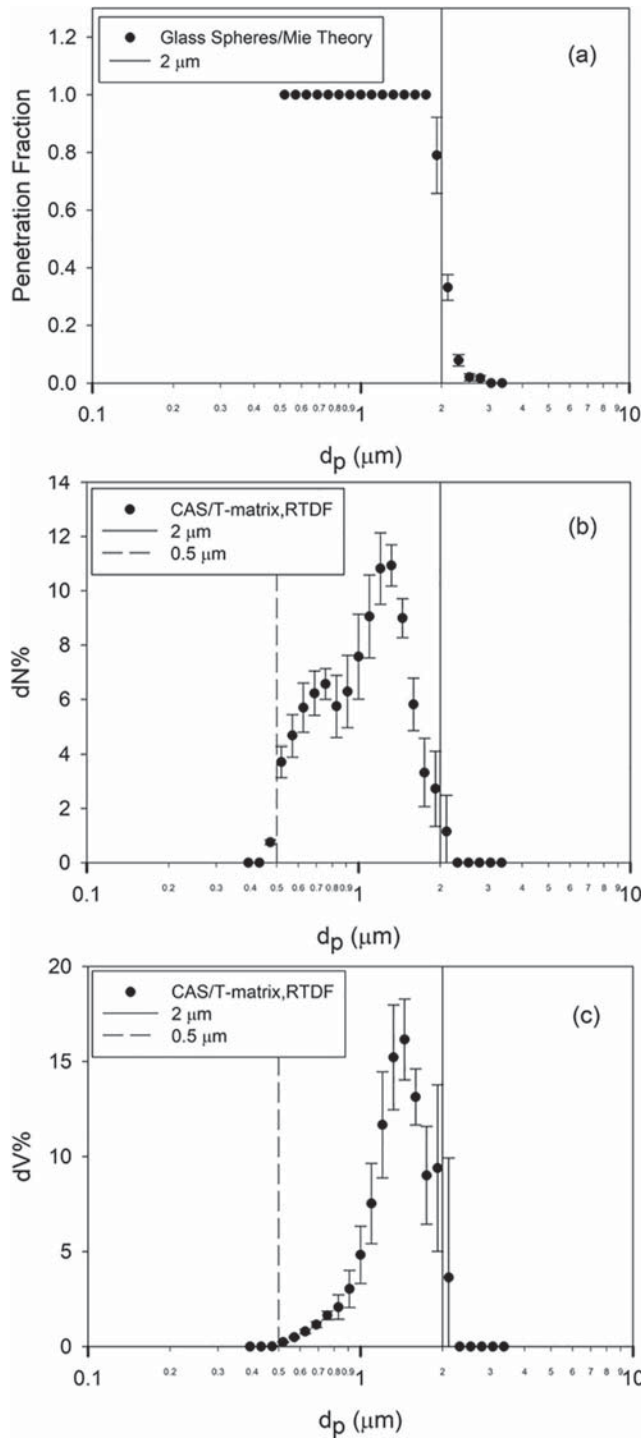
Fig. 8. (a) Fraction of glass spheres penetrating the high-flow rate cyclone downstream of the modified SSPD, which gave the test dust size range of sub-2 μm. Test coal dust (b) number-size and (c) volume-size distributions determined by CAS measurements and T-matrix and RTDF theory analyses. The dashed reference line represents the reported lower resolution of the CAS (Baumgardner et al. [28]).

tributing to this uncertainty were the uncertainty in glass sphere diameters, the variance in laser intensity, and electronic noise [53].

3.3. Calibration and comparison for test coal dust

CAS optical scattering cross section measurements were calibrated for bituminous coal dust using T-matrix (0.5–1.5 μm) and

RTDF (1.5–50 μm) theories. The size distribution resulting from the calibration was compared with a test dust produced by cyclone separation. A test dust of sub-2 μm was produced using a cyclone that removes 50% of 2.1-μm and 90% of 2.5-μm particles (Fig. 8a). Coal dust size computations agreed with the test dust size range—the number-size distribution shows that most particles were smaller than the cut-off diameter of 2.1 μm (Fig. 8b), and the volume-size distribution shows that the concentration decreased sharply at 2.1 μm (Fig. 8c). Near the lower size resolution, the number concentration was negligible at 0.4 μm and increased sharply at 0.5 μm (Fig. 8b). This increase coincides with the 0.5-μm lower resolution of the CAS given by Baumgardner and colleagues [28].

Coal dust size distribution computations were compared with the 3–20 μm test dust size range and with APS measurements. The coal dust size distribution agreed with the test dust size range given by the cyclone retention efficiency and sieve screen size (Fig. 9a). The distribution had a mass median diameter of 8.1 ± 0.1 μm and geometric standard deviation of 1.45 ± 0.04. The APS size distribution had a similar width (geometric standard deviation of 1.49 ± 0.01) but was shifted to smaller sizes (Fig. 9b). The mass median diameter of 7.1 ± 0.1 μm was 14% smaller than that of the CAS. The difference is not appreciable considering that the calibration for glass spheres had an uncertainty of 13% and this affected scattering cross section estimates for coal dust. The difference would have been greater if the measurements were not cali-
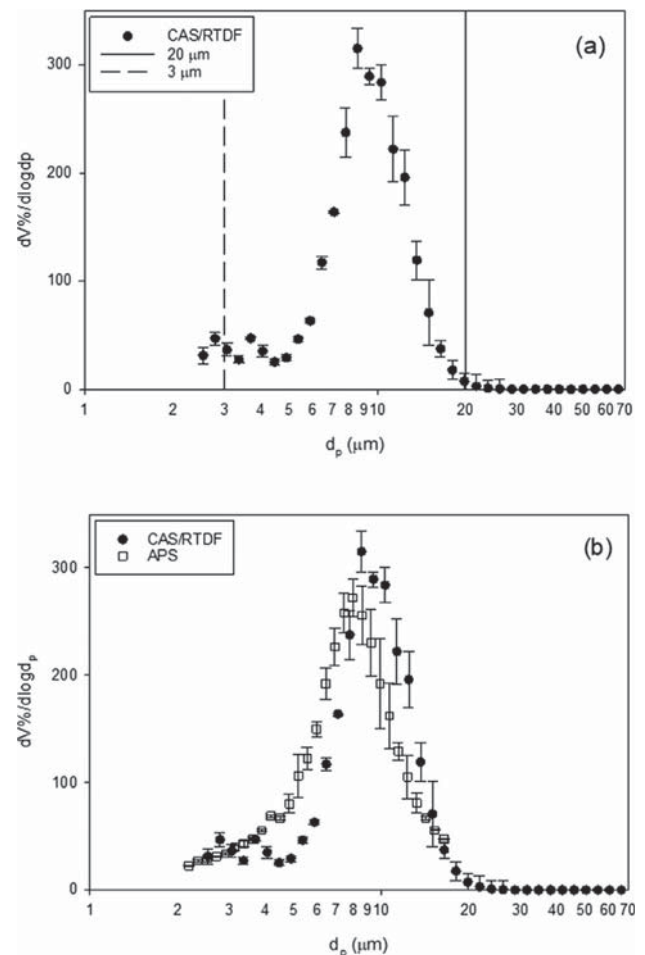

Fig. 9. Comparison of test coal dust (3–20 μm) volume-size distributions determined by CAS measurements and RTDF theory analysis (filled circles) with a) the cyclone cut-off and sieve size range (vertical lines) and b) APS measurements (open squares).
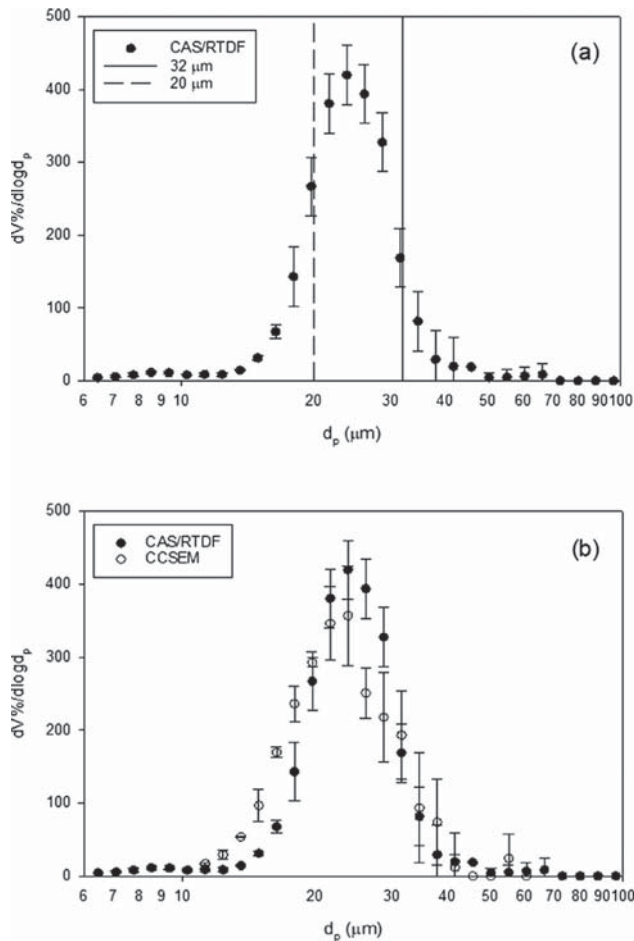
Fig. 10. Comparison of test coal dust (20–32 μm) volume-size distributions determined by CAS measurements and RTDF theory analysis (filled circles) with (a) the sieve size range (vertical lines) and (b) CCSEM measurements (open circles).

Fig. 11. Comparison of test coal dust (32–45 μm) volume-size distributions determined by CAS measurements and RTDF theory analysis (filled circles) with (a) the sieve size range (vertical lines) and (b) CCSEM measurements (open triangles).

brated for particle morphology. Specifically, a difference of 35% would have resulted from the improper assumption of spheres and the application of Mie theory [54] to estimate coal dust mass median diameter.

For the 20–32 μm test dust, the coal dust size distribution agreed well with the sieve size range and CCSEM measurements. The characteristic diameter was within the sieve size range and the distribution extended slightly outside (Fig. 10a) as expected for sieved powders [38,55]. The mass median diameter (22.9 ± 1.2 μm) measured by the CAS was only 5% larger than that measured by the CCSEM (21.9 ± 1.4 μm) (Fig. 10b). The similarity between the CAS and CCSEM distributions indicates the suitability of the calibration for this size range of coal dust. If spherical morphology were assumed and Mie theory were applied [54], the CAS estimate would have been 40% larger than the CCSEM measurement.

The coal dust size distribution for the 32–45 μm test dust was shifted to smaller sizes relative to the sieve size range (Fig. 11a). However, this shift was consistent with CCSEM measurements (Fig. 11b). The mass median diameter (29.7 ± 0.3 μm) measured by the CAS was only 4% larger than that of the CCSEM (28.5 ± 1.1 μm). The good agreement between CCSEM measurements and coal dust size distribution computations suggests that the calibration was accurate for large-size test dust. The difference between CAS and CCSEM measurements would have been 40% if spherical morphology were assumed and Mie theory were
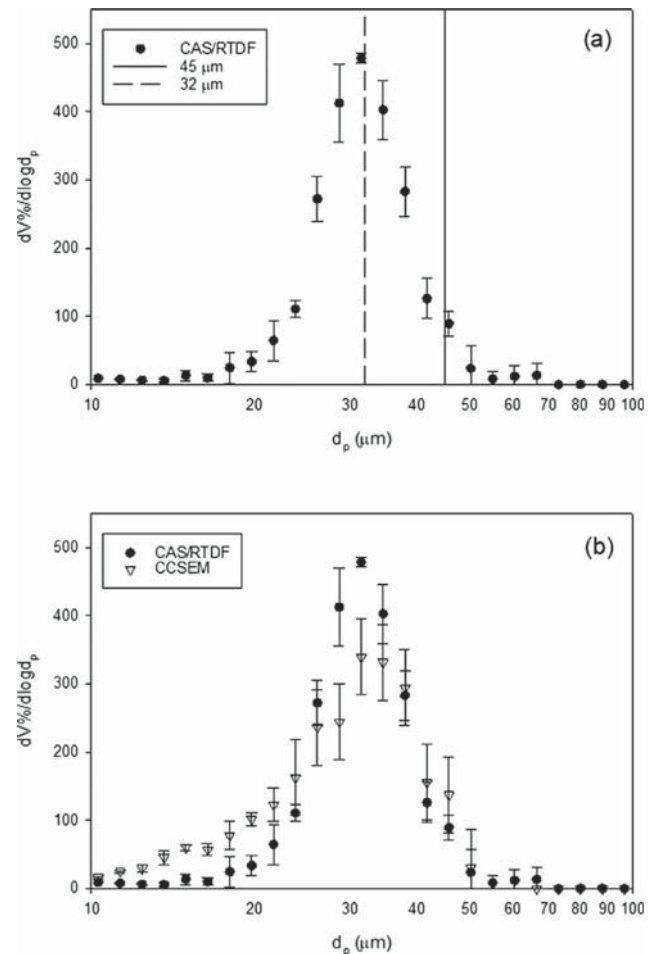
employed. Overall, coal dust diameters were up to 2.5 times larger than particle diameters determined by the manufacturer calibration for water droplets. The results suggest that the CAS calibration for particle composition and morphology prevented substantial under-sizing of coal dust relative to the manufacturer calibration for water and appreciable under-sizing of coal dust relative to the conventional calibration for spheres.

3.4. Comparison for bulk coal dust

The coal dust size distribution was determined for bulk dust following calibration of the CAS and sample de-agglomeration by the modified SSPD. The distribution was compared with conventional LD (Model LS 13 320, Beckman-Coulter, CA) measurements that utilized classical Mie theory [16,17]. The comparison shows a discrepancy between major modes of the number-size distribution (1.5 μm for the CAS and 0.5 μm for the LD) in Fig. 12a. In addition, the LD measured a broad volume-size distribution with a mode diameter of 23 μm, while the CAS measured a more narrow distribution with a mode diameter of 8.5 μm (Fig. 12b). The large difference between CAS and LD measurements can be attributed to differences in analytical techniques, but it also may be due to a lack of de-agglomeration by the LD inlet disperser. Because a coarse particle mode appears in the CAS number-size distribution at 8.5 μm, but one does not appear in the LD number-size distribution
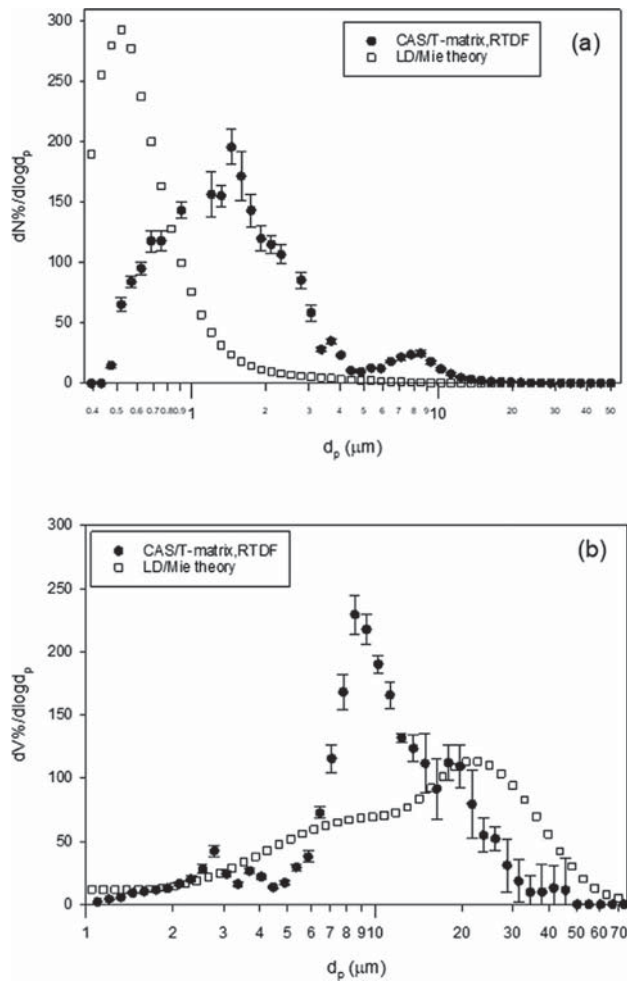
Fig. 12. Bulk coal dust (a) number-size distribution and (b) volume-size distribution estimated by CAS measurements and T-matrix and RTDF theory analyses for dust dispersed and de-agglomerated by the modified SSPD (filled circles), and LD and Mie theory analysis for bulk coal dust aerosolized by the LD inlet disperser (open squares).

at 23 μm (Fig. 12a), a lack of de-agglomeration by the LD inlet disperser may partially account for the discrepancy.

4. Conclusions

CAS measurements were calibrated by T-matrix and RTDF theories to account for effects of coal dust composition and morphology in size estimates. The calibration for composition prevented the underestimation of coal dust size by a factor of up to 2.5 relative to the manufacturer calibration for water. The calibration for morphology improved agreement with CCSEM and APS measurements. By accounting for elongation effects and assuming faceted shapes instead of smooth spheres, estimates for equivalent volume diameters were reduced. These reductions led to mass median diameters that were within 5% and 14% of CCSEM and APS measurements, respectively. The agreement was sufficient considering that the uncertainty in the basic calibration for glass spheres was 13% and this affected computations for coal dust. If spherical morphology were assumed and Mie theory were employed, CAS estimates would have been 40% and 35% larger than CCSEM and APS measurements, respectively.

Coal dust sizes determined from the calibration were also in agreement with test dust sizes generated by cyclone separation and air-jet sieving for particles in the range of 0.5–32 μm. For

32–45 μm, the computed size distribution contained particles smaller than the sieve size range. The presence of smaller particles and their significant contribution to the volume-size distribution were confirmed by CCSEM. Thus, the comparison with multiple sizing methods—cyclone separation, sieve segregation, CCSEM analysis, and APS measurements—suggested that the CAS can accurately measure coal dust diameters for studies on flammable dust control. This was the first study to show the suitability of the CAS for strongly light-absorbing, irregular particles. The measurements were facilitated by de-agglomerating powders for CAS analysis using the modified SSPD. Because LD volume-size distribution measurements were more than double that of the CAS, there may have been differences in de-agglomeration by the inlet dispersers. For the number-size distribution of bulk coal dust, LD gave a single mode at 0.5 μm, while the CAS gave a major mode at 1.5 μm and a minor mode at 8.5 μm. The differences between LD and CAS number-size distribution measurements should be explored further.

5. Disclaimer

The findings and conclusions in this paper are those of the authors and do not necessarily represent the official position of the National Institute for Occupational Safety and Health, Centers for Disease Control and Prevention. Mention of any company or product does not constitute endorsement by NIOSH.

Declaration of Competing Interest

None.

Acknowledgements

References

[1] Mine Safety and Health Administration: "Fatal Accident Report." (2011) Available at http://www.msha.gov/Fatals/2010/UBB/PerformanceCoalUBB.asp (accessed July 25, 2018).
[2] Harris, M., Cashdollar, K., Man, C. K. and Thimons, E. Mitigating Coal Dust Explosions in Modern Underground Coal Mines (2009). Available at SSRN: https://ssrn.com/abstract=3035297 or https://doi.org/10.2139/ssrn.3035297.
[3] Janisko, S.J., Colinet, J.F., Patts, J.R., Barone, T., Patts, L.D. Field Evaluation of an Inline Wet Scrubber for Reducing Float Coal Dust on a Continuous Miner Section. Presented at the 2015 SME Annual Meeting and Exhibit, February 15–February 18, Denver, Colorado, (2015) Pre-Print 15-031.
[4] J.R. Patts, J.F. Colinet, S.J. Janisko, T. Barone, L.D. Patts, Reducing float coal dust: field evaluation of an in-line auxiliary fan, Min. Eng. 68 (2016) 63–68.
[5] C.E. Seaman, M.R. Shahan, T.W. Beck, S.E. Mischler, Comparison of the CAS-POL and IOM samplers for determining the knockdown efficiencies of water sprays on float coal dust, J. Occup. Environ. Hyg. 15 (2018) (2018) 214–225.
[6] M. Hertzberg, K.L. Cashdollar, in: K.L. Cashdollar, M. Hertzberg (Eds.), Industrial Dust Explosions, American Society for Testing and Materials, Pennsylvania, 1987.
[7] Q. Li, K. Wang, Y. Zheng, M. Ruan, X. Mei, B. Lin, Experimental research of particle size and size dispersity on the explosibility characteristics of coal dust, Powder Technol. 292 (2016) 290–297.
[8] Y. Liu, P.H. Daum, The effect of refractive index on the size distributions and light scattering coefficients derived from optical particle counters, J. Aerosol Sci. 31 (2000) 945–957.
[9] P.W. Barber, S.C. Hill, Light scattering by particles: computational methods (Vol. 2), World Sci. (1990).

[10] B.Y.H. Liu, V.A. Marple, K.T. Whitby, N.J. Barsic, Size distribution measurement of airborne coal dust by optical particle counters, Am. Ind. Hyg. Assoc. J. 35 (1974) 443–451.

[11] K.T. Whitby, R.A. Vomela, Response of single particle optical counters to nonideal particles, Environ. Sci. Technol. 1 (1967) 801–814.

[12] R. Xu, Light scattering: a review of particle characterization applications, Particuology 18 (2015) 11–21.

[13] A.F. Silva, A. Burggraeve, Q. Denon, P. Van der Meeren, N. Sandler, T. Van Den Kerkhof, T. De Beer, Particle sizing measurements in pharmaceutical applications: comparison of in-process methods versus off-line methods, Eur. J. Pharm. Biopharm. 85 (2013) 1006–1018.

[14] G. Eshel, G.J. Levy, U. Mingelgrin, M.J. Singer, Critical evaluation of the use of laser diffraction for particle-size distribution analysis, Soil Sci. Soc. Am. J. 68 (2004) 736–743.

[15] Z. Ma, H.G. Merkus, J.G. de Smet, C. Heffels, B. Scarlett, New developments in particle characterization by laser diffraction: size and shape, Powder Technol. 111 (2000) 66–78.

[16] G. Mie, Beiträge zur Optik trüber Medien speziell kolloidaler Metallösungen, Ann. Phys. 25 (1908) 377–445.

[17] C.F. Bohren, D.R. Huffman, Absorption and scattering of light by small particles, Wiley, New York, 1983.

[18] S.J. Blott, K. Pye, Particle size distribution analysis of sand-sized particles by laser diffraction: an experimental investigation of instrument sensitivity and the effects of particle shape, Sedimentology 53 (3) (2006) 671–685.

[19] M. Naito, O. Hayakawa, K. Nakahira, H. Mori, J. Tsubaki, Effect of particle shape on the particle size distribution measured with commercial equipment, Powder Technol. 100 (1) (1998) 52–60.

[20] B. Wilson, T. Dewers, Z.E. Reches, J. Brune, Particle size and energetics of gouge from earthquake rupture zones, Nature 434 (7034) (2005) 749.

[21] R.N. Kelly, K.J. DiSante, E. Stranzl, J.A. Kazanjian, P. Bowen, T. Matsuyama, N. Gabas, Graphical comparison of image analysis and laser diffraction particle size analysis data obtained from the measurements of nonspherical particle systems, AAPS Pharm. Sci. Tech. 7 (2006) E93–E106.

[22] E.J. Garboczi, K.A. Riding, M. Mirzahosseini, Particle shape effects on particle size measurement for crushed waste glass, Adv. Powder Technol. 28 (2) (2017) 648–657.

[23] D.L. Jaggard, C. Hill, R.W. Shorthill, D. Stuart, M. Glantz, F. Rosswog, B. Taggart, S. Hammond, Light scattering from particles of regular and irregular shape, Atmos. Environ. 15 (1981) 2511–2519.

[24] J.S. Reid, H.H. Jonsson, H.B. Maring, A. Smirnov, D.L. Savoie, S.S. Cliff, E.A. Reid, J. M. Livingston, M.M. Meier, O. Dubovik, S.C. Tsay, Comparison of size and morphological measurements of coarse mode dust particles from Africa, J. Geophys. Res. Atmos. 108 (2003) D19.

[25] A.A. Kokhanovsky, Optical properties of irregularly shaped particles, J. Phys. D Appl. Phys. 36 (7) (2003) 915.

[26] Y. Okada, Numerical simulations of light scattering and absorption characteristics of aggregates, Light Scattering Reviews, vol. 5, Springer, Berlin, Heidelberg, 2010, pp. 3–35.

[27] D. Baumgardner, H. Jonsson, W. Dawson, D. O'Connor, R. Newton, The cloud, aerosol and precipitation spectrometer: a new instrument for cloud investigations, Atmos. Res. 59 (2001) 251–264.

[28] D. Baumgardner, J.L. Brenguier, A. Bucholtz, H. Coe, P. DeMott, T.J. Garrett, M. Krämer, Airborne instruments to measure atmospheric aerosol particles, clouds and radiation: a cook's tour of mature and emerging technology, Atmos. Res. 102 (2011) 10–29.

[29] B. Johnson, K. Turnbull, P. Brown, R. Burgess, J. Dorsey, A.J. Baran, E. Hesse, In situ observations of volcanic ash clouds from the FAAM aircraft during the eruption of Eyjafjallajökull in 2010, J. Geophys. Res. Atmos. 117 (2012) D20.

[30] E. Hesse, D.S. McCall, Z. Ulanowski, C. Stopford, P.H. Kaye, Application of RTDF to particles with curved surfaces, J. Quant. Spect. Rad. Trans. 11 (2009) 1599–1603.

[31] S. Havemann, A.J. Baran, Extension of T-matrix to scattering of electromagnetic plane waves by non-axisymmetric dielectric particles: application to hexagonal ice cylinders, J. Quant. Spectrosc. Radiat. Transfer 70 (2001) 139–158.

[32] W.C. Conant, T.M. VanReken, T.A. Rissman, V. Varutbangkul, H.H. Jonsson, A. Nenes, R.C. Flagan, Aerosol-cloud drop concentration closure in warm cumulus, J. Geophys. Res. Atmos. 109 (2004) D13.

[33] S. Lance, Coincidence errors in a cloud droplet probe (CDP) and a cloud and aerosol spectrometer (CAS), and the improved performance of a modified CDP, J. Atmos. Oceanic Technol. 29 (2012) 1532–1541.

[34] A. Macke, J. Mueller, E. Raschke, Single scattering properties of atmospheric ice crystals, J. Atmos. Sci. 53 (1996) 2813–2825.

[35] S.R. Osborne, A.J. Baran, B.T. Johnson, J.M. Haywood, E. Hesse, S. Newman, Short-wave and long-wave radiative properties of Saharan dust aerosol, Q. J. R. Meteorol. Soc. 137 (2011) 1149–1167.

[36] J.T. McCartney, J.B. Yasinsky, S. Ergun, Optical constants of coals by reflectance measurements in the ultra-violet and visible spectrum, Fuel 44 (1965) 349–354.

[37] T.C. Bond, R.W. Bergstrom, Light absorption by carbonaceous particles: an investigative review, Aerosol. Sci. Technol. 40 (2006) 27–67.

[38] H.G. Merkus, Sieves and sieving, Particle Size Measurements vol. 17 (2009).

[39] H. Polat, M. Polat, S. Chander, R. Hogg, The electrostatic charge on particles and its relation to agglomeration in air, Appl. Occup. Environ. Hyg. 11 (1996) 817–825.

[40] B.T. Chen, H.C. Yeh, B.J. Fan, Evaluation of the TSI small-scale powder disperser, J. Aerosol Sci. 26 (1995) 1303–1313.

[41] W.C. Hinds, Aerosol technology: properties, behavior, and measurement of airborne particles, John Wiley & Sons, Inc., New York, 1999, pp. 54, 406.

[42] C.N. Davies, Particle-fluid interaction, J. Aerosol. Sci. 10 (1979) 477–513.

[43] H. Huang, K. Wang, D.M. Bodily, V.J. Hucka, Density measurements of Argonne premium coal samples, Energy Fuels 9 (1995) 20–24.

[44] P.A. Baron, Calibration and use of the aerodynamic particle sizer (APS 3300), Aerosol. Sci. Technol. 5 (1986) 55–67.

[45] P.A. Jaques, P.K. Hopke, P. Gao, Quantitative analysis of unique deposition pattern of submicron Fe_3O_4 particles using computer-controlled scanning electron microscopy, Aerosol. Sci. Technol. 46 (2012) 905–912.

[46] R.D. Willis, F.T. Blanchard, T.L. Conner, Guidelines for the Application of SEM/ EDX Analytical Techniques to Particulate Matter Samples. EPA No. 600/R-02/ 070. US Environmental Protection Agency, Research Triangle Park, NC (2002).

[47] Y. Mamane, R. Willis, T. Conner, Evaluation of computer controlled scanning electron microscopy applied to an ambient urban aerosol sample, Aerosol. Sci. Technol. 34 (2001) 97–107.

[48] P.K. Hopke, G.S. Casuccio, Scanning electron spectroscopy, in: P.K. Hopke (Ed.), Receptor Modeling for Air Quality Management, Elsevier Science, Amsterdam, 1991, pp. 149–212.

[49] J.P. Mathews, S. Eser, P.G. Hatcher, A.W. Scaroni, The shape of pulverized bituminous vitrinite coal particles, KONA 25 (2007) 145–152.

[50] V. Timbrell, The terminal velocity and size of airborne dust particles, Brit. J. Appl. Phys. 5 (1954) S86.

[51] L. Jianzhong, Z. Weifeng, Y. Zhaosheng, Numerical research on the orientation distribution of fibers immersed in laminar and turbulent pipe flows, J. Aerosol. Sci. 35 (2004) 63–82.

[52] T.L. Barone, E. Hesse, C.E. Seaman, A.J. Baran, T.W. Beck, M.L. Harris, P.A. Jaques, P. Gao, D.E. Schwegler-Berry, S.E. Mischler, Real-time sizing of airborne coarse coal dust, Society for Mining, Metallurgy, and Exploration, 2017.

[53] D. Baumgardner, H. Chepfer, G.B. Raga, G.L. Kok, The shapes of very small cirrus particles derived from in situ measurements, Geophys. Res. Lett. 32 (1) (2005).

[54] M.I. Mishchenko, J.M. Dlugach, E.G. Yanovitskij, N.T. Zakharova, Bidirectional reflectance of flat, optically thick particulate layers: an efficient radiative transfer solution and applications to snow and soil surfaces, J. Quant. Spectrosc. Radiat. Transfer 63 (1999) 409–432.

[55] P.D. Komar, B. Cui, The analysis of grain-size measurements by sieving and settling-tube techniques, J. Sediment. Res. 54 (1984) 2.